Adsorption (2007) 13: 439–451
DOI 10.1007/s10450-007-9036-2

Adsorption of n-alkanes in faujasite zeolites: molecular simulation study and experimental measurements

A. Wender · A. Barreau · C. Lefebvre · A. Di Lella · A. Boutin · P. Ungerer · A.H. Fuchs

Received: 30 April 2007 / Revised: 23 July 2007 / Accepted: 24 July 2007 / Published online: 22 September 2007

Abstract We report an application of a previously developed force field for adsorption of hydrocarbons in silicalite (Pascual, P., et al. in Phys. Chem. Chem. Phys. 5:3684–3693, 2003), to the case of the linear alkane-sodium faujasite systems. In order to extend this force field from siliceous to cationic zeolites, we propose to take into account the polarization part of the zeolite-molecule interaction energy. A first order polarization term is explicitly considered for this purpose, using standard molecular polarizabilities. Polarization appears to amount to 30–40% of the zeolite-alkane interaction energy, as a consequence of the strong electric field created by the sodium cation distribution and negatively charged framework. This approach is compared with experimental adsorption isotherms of ethane, propane, n-octane and n-decane in NaY from the literature and with original measurements of n-butane isotherms in NaY obtained by thermal gravimetry. Henry constants and heats of adsorption at zero coverage of n-alkanes ($n = 6$–10) are also compared with experimental measurements. Although no specific parameter has been calibrated for extending the force field, the general agreement between simulation results and experiments is satisfactory. Cation redistribution upon alkane adsorption is not observed in these simulations.

A. Wender · A. Barreau · C. Lefebvre · P. Ungerer
IFP, 1-4 avenue de Bois Préau, 92852 Rueil-Malmaison Cedex, France

A. Di Lella · A. Boutin (✉)
Laboratoire de Chimie Physique, Bâtiment 349, UMR 8000 CNRS, Université de Paris-Sud, 91405 Orsay, France
e-mail: anne.boutin@lcp.u-psud.fr

A.H. Fuchs
Ecole Nationale Supérieure de Chimie de Paris (ENSCP), 11 rue Pierre et Marie Curie, 75231 Paris Cedex 05, France

Keywords Adsorption · Alkanes · Zeolites · Faujasites · Grand Canonical Monte Carlo Simulation

Abbreviations

a_i	Torsion parameters
A	Parameter of Henry constant expression, mol/kg/Pa
B	Parameter of Henry constant expression
E_i	Local electrical field, J/mol
ΔG	Gibbs free energy, kJ/mol
ΔH_0	Heat of adsorption, kJ/mol
$\Delta S_{0,local}$	Entropy of adsorption at low coverage, kJ/mol/K
f_i	Fugacity of molecule i, Pa
k	Ideal gas constant, J/mol/K
K_H	Henry constant, mol/kg/Pa
K'	preexponential factor, mol/kg/Pa
N	Number of adsorbed molecules
N_i	Number of adsorbed molecules i
p^θ	Standard pressure, bar
r_{ij}	Distance between two centres of force i and j, Å
T	Temperature, K
U_{bend}	Bond-bending interaction, J/mol
$\bar{U}_{ext\_new}$	Lennard Jones energy obtained with the United Atom model, J/mol
U^s_{ext}	Intermolecular interactions in the adsorbed phase, J/mol
U_{intra}	Intramolecular interaction, J/mol
U_{LJ}	Lennard-Jones potential, J/mol
U_{pol}	Polarization energy, J/mol
U_{tors}	Torsion interaction, J/mol
V	Unit volume, Å^3
W_{new}	Rosenbluth factor

Greek letters

σ_i	Lennard-Jones parameter of the centre of force i, Å
ε_i	Lennard-Jones parameter of the centre of force i, K
σ_{ij}	Crossing Lennard-Jones parameter between the centre of force i and j, Å
ε_{ij}	Crossing Lennard-Jones parameter between the centre of force i and j, K
θ	Bending angle, degree
ϕ	Dihedral angle, degree
α_p	Polarizability tensor
$\bar{\mu}_i$	Chemical potential
n_T	Number of adsorption sites

1 Introduction

In aluminosilicate faujasite-type zeolite, a detailed knowledge of the adsorption mechanism of hydrocarbons is of great interest in the context of petrochemical application such as separation processes. A prominent application is the separation of branched alkanes from n-alkanes, aimed at producing fuels of high octane number. Molecular simulation can be used to understand the adsorption phenomenon of pure components and the separation mechanism of fluid mixtures at the microscopic level and to increase industrial process performances.

Computer simulation studies on the adsorption of molecules in cation-exchanged faujasite-type zeolite have been performed in the case of halocarbons (Mellot and Cheetham 1999), aromatics (Gener et al. 2000; Lachet et al. 1998, 1999, 2001) and hydrocarbons (Pascual et al. 2005; Dubbeldam et al. 2004; Beerdsen et al. 2002, 2003; Calero et al. 2004). Calero et al. (2004) computed the adsorption isotherms, Henry constants and heats of adsorption at low coverage of linear alkanes in NaY (methane, ethane, propane) and in NaX (methane, ethane, propane, n-butane, n-pentane, n-decane) using Grand Canonical Monte Carlo simulations. They have developed a United Atom force field for alkanes (centres of force CH_4, CH_3 and CH_2) and used Lennard-Jones and coulombic potentials to model the interaction between atomic or molecular species. The alkane-sodium, alkane-alkane and alkane-framework interaction parameters were obtained by calibrating the force field through explicitly fitting a full isotherm over a wide range of pressures, temperatures, and sodium densities.

Following up on our previous studies of hydrocarbon adsorption in various zeolites (Pascual et al. 2003, 2004; Bourasseau et al. 2002a, 2002b, 2003), our aim is to develop a general (transferable) hydrocarbon adsorption model, encompassing purely siliceous (silicalite, ferrierite) and cationic (faujasite) zeolites with a unique parametrization. We use the force field for the alkane-siliceous zeolite systems of Pascual et al. (2003) in which the framework oxygen σ (3.0 Å) and ε (93.53 K) Lennard-Jones parameters were calibrated using the experimental adsorption isotherms of n-butane in silicalite-1 at 277 K and 373 K. This force field was successfully tested for the alkane-ferrierite system, without any further parameter readjustment (Pascual et al. 2004).

We report here an extension of this force field to n-alkane adsorption in sodium-faujasite. The main question that has to be addressed in this case is how to take into account the polarization part of the zeolite-molecule interaction energy that arises from the strong electric field created by the sodium cation distribution. Polarization effects are usually not taken into account in the molecular simulation studies of adsorption in siliceous zeolites (Fuchs and Cheetham 2001). While Calero and coworkers included polarization effects in an effective manner (Calero et al. 2004), we report here an attempt to explicitly account for these effects. Following Pascual et al. (2003), we combine the zeolite parameters with adsorbate-adsorbate anisotropic united atom (AUA-4) parameters (Ungerer et al. 2000) to yield adsorbent-adsorbate parameters. The Lorentz–Berthelot combining rules are used to obtain cross potential parameters from the individual molecular group values.

Few experimental data are available for adsorption of hydrocarbons in Faujasite zeolites. For the adsorption of n-alkanes in NaY faujasites, experimental isotherms are available for ethane, propane (Hampson and Rees 1993), n-hexane (Ramachandran et al. 2005), n-octane and n-decane (Denayer and Baron 1997). Adsorption equilibria of hydrocarbons on dealuminated faujasites have also be measured (see for instance the review of Stach et al. 1986). In order to increase this experimental data base, original adsorption isotherms of n-butane in a faujasite Y with 52 sodium per unit cell (Si:Al = 2.7) have been measured at IFP (Institut Français du Pétrole).

In the second section of this article, we present the experimental method for measuring the adsorption isotherms, its validation with literature data and the original adsorption isotherms of n-butane in NaY. The third section is devoted to the zeolite structure models used in this study as well as to the simulation methods used to obtain adsorption isotherms, Henry constants, heats of adsorption and cation location. The last section is devoted to the comparison of simulation results with experimental data and to their discussion.

2 Experimental section

2.1 Materials

The adsorbent used was NaY zeolite in the form of powder supplied by CECA Co., France with a high crystallinity of

100%, determined by X-ray diffraction by comparison with a reference sample. The Si:Al ratio measured by X-ray fluorescence is 2.7.

The silicalite used for validating the experimental procedure was supplied in the form of powder by Zeolist, USA. The average crystal size was ∼1.5 μm. The cristallinity rate determined by X-ray diffraction by comparison with a reference sample is 98%. The Si:Al ratio measured by X-ray fluorescence is 507. Normal butane was purchased from Air Liquide (France) with a purity of 99.99%.

2.2 Apparatus and procedure

Adsorption measurements were carried out gravimetrically by using a SETARAM symmetrical electromagnetic suspension microbalance (model TAG 24). It has a 0.1 μg resolution and a 1 μg precision for a measuring full scale of 100 mg. The n-butane partial pressures were obtained by helium dilution (Sun et al. 1998) at atmospheric pressure by means of different range mass flow controllers.

In a typical experiment, about 20 mg of the sample zeolite was preliminarily activated at 653 K under helium flow. The temperature was raised at a rate of 10 K/mn and maintained at the highest temperature during 16 hours. Then temperature was decreased to the desired temperature at a rate of 5 K/mn. The equilibrium time was fixed to 10 hours, this time is more than enough to establish sorption equilibrium in this system.

2.3 Validation and results

The experimental procedure has been validated by the adsorption measurements of n-butane in silicalite-1. In Fig. 1, the adsorbed amounts of n-butane measured on silicalite are compared with the data from Sun et al. (1998) at 350 K and Abdul-Rehman et al. (1990) at 353 K. At 350 K, the adsorption isotherm of n-butane is in a good agreement with Sun et al. The data from Abdul-Rehman et al. are significantly lower than our results but, as mentioned by Sun et al., this may be explained by the use of silicalite pellets by Abdul-Rehman et al. The adsorbed amounts of n-butane at 343 K and 423 K on NaY faujasite are indicated in Table 1.

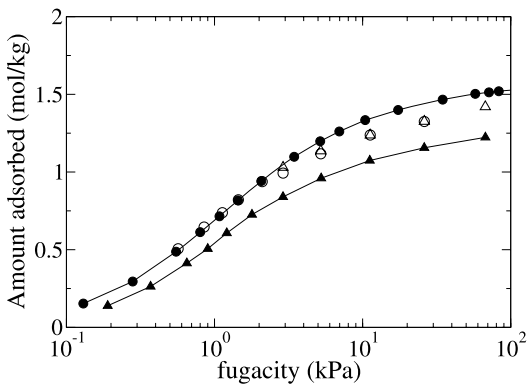

Fig. 1 Adsorption isotherm of n-butane in silicalite-1 at 353 K (*circles*) and 350 K (*triangles*). This work (*open symbols*) and literature data (*filled symbols*) (Sun et al. 1998; Abdul-Rehman et al. 1990)

3 Model and methodology

3.1 Sodium faujasite model

The crystal structure of faujasite was taken from X-ray diffraction experiments (Fitch et al. 1986). The crystal solid is described in the F3d symmetry group with a cubic cell parameter of 24.8536 Å. As in most of our previous studies, we used an average "T-atom" to average over all possible Al location for a given Si:Al ratio. Any explicit Al distribution would require much larger systems in order to avoid non-physical periodic effects, caused by the limited number of unit cells used in the periodic simulation box (Ungerer et al. 2005). In previous studies, Beauvais et al. (2004) have generated the right sodium location in faujasite, using such an average model. An explicit account of Si and Al location in the model was found to have a rather weak effect on the extraframework cation distributions. The partial electrostatic charges for the framework atoms were determined from the work of Mortier (Uytterhoeven et al. 1992) as in previous studies (Beauvais et al. 2004) (Table 2).

The cation distribution in faujasite is usually described as follows. Na^+ can occupy sites I, located in the hexagonal prism which connects the sodalite cages. Sites I' are inside the sodalite cages facing sites I. Sites II are in front of the hexagonal windows inside the supercages. Sites III are also

Table 1 Experimental adsorption isotherm of n-butane on Na-Y zeolite at 343 K and 423 K

T = 343 K		T = 423 K	
P^a/kPa	Q^b/mol·kg^{-1}	P^a/kPa	Q^b/mol·kg^{-1}
0.57	0.87	0.56	0.18
0.90	1.16	0.95	0.22
1.65	1.65	1.29	0.25
2.12	1.85	2.12	0.31
3.17	2.11	3.16	0.38
5.35	2.34	5.29	0.76
10.7	2.57	10.5	1.13
20.9	2.72	20.5	1.58
36.8	2.85	35.8	1.87
63.1	2.97	62.2	2.13
82.6	3.05	81.0	2.26

[a] P is the partial pressure of n-butane

[b] Q is the adsorbed amount

Table 2 Partial charges for the framework atoms in the faujasites $Na_{52}Y$ (Si:Al = 2.69) and $Na_{56}Y$ (Si:Al = 2.43)

Number of cations per unit cell	$q_{\text{T-atom}}/\lvert e\rvert$	$q_O/\lvert e\rvert$	$q_{Na}/\lvert e\rvert$
52	+1.3796	−0.82525	+1
56	+1.3633	−0.82750	+1

Table 3 Cation distribution for the two faujasite models (number of cations per unit cell)

Sites	I	I'	II	III
$Na_{52}Y$	12	8	32	0
$Na_{56}Y$	8	16	32	0

in the supercages, near the 4 membered rings of the sodalite cages. Sites I have a multiplicity of 16 per unit cell, sites I' and II have a multiplicity of 32, and sites III have a multiplicity of 48 per unit cell. Sites III are reported to be of higher potential energy than sites I, I' and II (Beauvais et al. 2004). At low occupancy (Si:Al > 1.5), cations are known to occupy sites I, I' and II only (Vitale et al. 1997).

The cation distributions for the dehydrated faujasite models are taken from Beauvais et al. (2004) simulation studies and they are given in Table 3. In most of the present simulations, we consider the zeolite structures with a fixed cation distribution. In order to examine the possible extraframework cation redistribution upon alkane adsorption (a feature that was reported by Calero et al. 2004), we have undertaken a simulation of n-octane adsorption in $Na_{52}Y$ at 598 K, in which the sodium cations are free to move.

3.2 Forcefield

Following Ungerer and coworkers (Ungerer et al. 2000; Bourasseau et al. 2002a, 2002b, 2003), n-alkanes are described within the anisotropic united atom (AUA-4) model where CH_3 and CH_2 groups are represented with a single centre of force located near the geometric centre of the atoms of each group. Intermolecular interactions (1) are described by a Lennard-Jones 6–12 potential and the parameters are given in Table 4:

$$U_{LJ}(r_{ij}) = 4\varepsilon_{ij}\left[\left(\frac{\sigma_{ij}}{r_{ij}}\right)^{12} - \left(\frac{\sigma_{ij}}{r_{ij}}\right)^{6}\right]. \quad (1)$$

Intramolecular interactions (2) include bond-bending (3) and torsion (4) potentials as well as non-bonded interactions described by a Lennard-Jones 6–12 potential (1):

Table 4 Force field parameters for the interactions between alkane force centres and the zeolite in the AUA model. δ is the offset distance between the force centre and the carbon nucleus toward the group centre of mass and α_p is the polarizability of the different centres of force

		σ/Å	(ε/k)/K	δ/Å	Polarizability α_p/Å^3
Sorbate	CH_2	3.4612	86.29	0.38405	2.22
	CH_3	3.6072	120.15	0.21584	1.78
Zeolite	O	3.0	93.53	0.0	/
	Na	2.584	50.34	0.0	/

Table 5 Set of parameters for intramolecular potential, the letter i is used to indicate either a CH_3 or a CH_2 group, i.e. $i = 2, 3$

Molecular weight/g·mol^{-1}	CH_3	15.03	
	CH_2	14.03	
C-C distance/Å		1.535	
Bending	C-CH_2-C	$\theta_0/°$	114
		k_{bend}/K	74900
	C-CH-C	$\theta_0/°$	112
		k_{bend}/K	72700
Torsion	CH_i-CH_2-CH_2-CH_i	a_0/K	1001.35
		a_1/K	2129.52
		a_2/K	−303.06
		a_3/K	−3612.27
		a_4/K	2226.71
		a_5/K	1965.93
		a_6/K	−4489.34
		a_7/K	−1736.22
		a_8/K	2817.37

$$U_{intra}(mol) = \sum_{i=2}^{N_{cf}(mol)-1} U_{bend}(\theta_i) + \sum_{i=2}^{N_{cf}(mol)-2} U_{tors}(\phi_i) + \sum_{i=1}^{N_{cf}(mol)-4} \sum_{j=i+4}^{N_{cf}(mol)} U_{LJ}(r_{ij}) \quad (2)$$

where

$$U_{bend}(\theta_i) = k_\theta(\cos(\theta_i) - \cos(\theta_0))^2/2, \quad (3)$$

$$U_{tors}(\phi_i) = \sum_{i=0}^{8} a_i \cos^i(\phi). \quad (4)$$

The parameter values are given in Tables 4 and 5.

The unlike interatomic interaction parameters are calculated by using the Lorentz–Berthelot combining rules, i.e. a geometric combining rule for the energy and an arithmetic combining rule for the atomic size:

$$\varepsilon_{ij} = \sqrt{\varepsilon_i \varepsilon_j}, \quad (5)$$

$$\sigma_{ij} = \frac{\sigma_i + \sigma_j}{2}. \quad (6)$$

The dispersion-repulsion part of the guest-host interactions is also described by a Lennard-Jones potential and the Lorentz–Berthelot combination rules, using the parameters of Pascual et al. (2003) for zeolite oxygens, and the parameters of Dang (1995) for sodium cations (determined in aqueous liquid in which cation-oxygen interactions are taken into account). Within the so-called Kiselev model (Fuchs and Cheetham 2001; Boutin et al. 2001), the sorbate/zeolite interactions are dominated by interactions between the guest molecules and the host oxygen atoms, so that the Si and Al framework atoms are not considered explicitly in dispersion-repulsion interactions.

Coulombic terms, that act between all partial charges of the framework and the +1 charge of the sodium cations, are considered only when cation mobility is investigated.

We explicitly compute the first term of the polarization energy development, through

$$U_{pol} = -\frac{1}{2} \sum_i E_i \cdot \alpha_p \cdot E_i \quad (7)$$

where α_p is the polarizability tensor and E_i is the local electrical field value at the polarization point of molecule i due to the charges on faujasite framework obtained using the Ewald summation technique. The back polarization effect (second term of the polarization energy development) induced by the guest molecules is weak enough in these systems (1–2% of the first term) to be neglected in the simulations (Frenkel and Smit 1996).

The distribution of polarizable sites was derived in the following way. Molecular polarizabilities are known to be additive in the sense that the mean polarizability of a molecule can be expressed as a sum of contributions from its individual atoms or functional groups. In this work, we do not consider the possible anisotropy of the polarizability tensor, and the polarizable sites are located on the Lennard-Jones anisotropic united atom sites. We have used the polarizability values assigned by Delhommelle et al. (2000) for CH_3 and CH_2 centres (Table 4).

In order to study the interplay between cation mobility and alkane adsorption, we used the potential developed by Jaramillo and Auerbach (1999) for the interactions between the sodium cations and the faujasite framework. This potential consists of an exponential-6 dispersion-repulsion term between the cation and the oxygen atoms of the zeolite (Na-O parameters: $\alpha = 61 \times 10^6$ K; $\beta = 4.05$ Å; $\gamma = 76.52 \times 10^4$ K Å^6), and a coulombic term between the cations and the framework atoms (oxygen and T atoms). The cation-cation interactions are described by a coulombic term only.

3.3 Monte Carlo Simulation methods

Adsorption isotherms were computed using biased grand canonical ensemble (Frenkel and Smit 1996) (μ, V, T) Monte Carlo simulations. The simulation box is composed of eight unit cells of faujasite (8 sodalite cages and 8 supercages) with periodic boundary conditions. The zeolite framework is considered as rigid and the guest-host interactions are calculated on a grid of points prior to simulations. The grid mesh is about 0.2 Å. Intermolecular interactions are calculated with a cut-off distance fixed at 12.42 Å.

In order to accelerate the convergence of the simulation runs, we used pre-insertion (Loyens et al. 1995) and configurational bias moves (Smit and Maesen 1995; Smit et al. 1995) for the molecular insertion and deletion Monte Carlo moves. Translation and rotation moves allow a displacement and a rotation of an entire molecule without changing its internal geometry respectively. Flip (Marantzas and Theodorou 1998), regrowth and reptation moves (Vacatello et al. 1980; Boyd 1989) were used to change internal conformation and to displace a part of a molecule inside zeolite pores. The flip move consists of choosing a CH_2 force centre along the chain and to rotate it according to an axis joining its immediate neighbours. The maximum amplitude of translations, rotations and flips was determined in such a way that 50% of the attempted moves were accepted. The regrowth move is based on configurational bias Monte Carlo or CBMC (Frenkel and Smit 1996; Smit and Siepmann 1994). This bias (Smit et al. 1995; Pablo et al. 1992) takes advantage of the flexibility of the molecule to grow step by step the part of the molecule to be changed, testing several possible random locations r_k, $k = l, \ldots, k_{max}$ for the next force centre. The partial regrowth using the configurational bias algorithm was adapted to the anisotropic united atom. The reptation move, which is also using the configurational bias, mimics the translation of a chain in a pore by suppressing one or several force centres from one end of the chain and to add them to the other end. Insertion and deletion moves are attempted in order to allow the number of molecules inside the zeolite to fluctuate also using the CBMC procedure. Each move has an occurrence probability which depends on the alkane considered (see Table 6). Grand canonical Monte Carlo simulations were performed during 2 million steps in order to equilibrate the system, followed by 20 million steps for the statistical averages.

For the cation mobility, we use conventional translation moves, as discussed above, and a biased translational jump move at new randomly selected positions. The jump move consists in deleting a cation at random, and to insert it back in the available porous volume at a position chosen among k trial positions ($k = 10$). It is thus somewhat equivalent to a translation move in which the maximum amplitude would not be limited. In the case of cations in zeolites, this move

Table 6 Probability of occurrence (%) for each Monte Carlo move during simulation

	Translation	Rotation	Flip	Reptation	Regrowth	Insertion/ deletion
C_2-C_3	30	20	–	–	–	50
C_4-C_6	25	20	–	–	10	45
C_7-C_8	25	20	–	–	20	35
C_9-C_{10}	15	15	10	15	15	30

is particularly useful because it provides site to site hopping without the penalty of exploring intermediate positions of high energy. In the anhydrous zeolite, the jump move permits to obtain the distribution of cations in equilibrium conditions consistently with previous simulations by Beauvais et al. (2004) in faujasites $Na_{52}Y$ (Si:Al = 2.69) and $Na_{56}Y$ (Si:Al = 2.43) (see Table 3).

3.4 Henry constants

In the case of adsorption at low coverage such that all molecules are isolated from their nearest neighbours, the equilibrium relationship between gas pressure and adsorbed amount is known to be linear. The Henry constant of adsorption K_H is defined in the limit of low coverage by the following equation:

$$K_H = \frac{\langle N_i \rangle}{V \cdot f_i} \tag{8}$$

where $\langle N_i \rangle / V$ is the average number of adsorbed molecules per unit volume (molecule/Å^3) and f_i is the fugacity in equilibrium conditions (Pa). The fugacity is obtained by the following relationship:

$$f_i = P_0 \exp\left(\frac{\bar{\mu}_i}{kT}\right) \tag{9}$$

where $\bar{\mu}_i$ is the chemical potential expressed with the classical reference state, i.e. a perfect gas of pure component i under a pressure P_0 equal to 1 Pa and a temperature T.

The determination of Henry constant makes use of the chemical potential evaluated by Widom test insertions in an empty zeolite associated to a configurational bias. The basic idea of the Widom test is to try to insert a ghost molecule at a random position and this molecule is assumed to have no influence on the rest of the system. The chemical potential is computed using biased NVT ensemble simulation and is expressed by Ungerer et al. (2005):

$$\bar{\mu}_i = -kT \ln\left\langle \frac{P_0 V W_{new}}{kT(N_i+1)} \exp(\beta \bar{U}_{ext\_new} - \beta U_{ext\_new}) \right\rangle \tag{10}$$

where the subscript *new* refers to the molecule that is tentatively inserted, W_{new} is the Rosenbluth factor of the new configuration, $\bar{U}_{ext\_new}$ the external energy obtained with a modified force field during the regrow process, U_{ext_new} the true full energy obtained with Anisotropic United Atom model. For Widom test insertion in an empty zeolite, the current number of molecules N_i is set to 0.

When regrowing the end of the chain from an atom n to the atom m, the Rosenbluth factor of the new configuration is calculated according to:

$$W_{new} = \prod_{l=n}^{m} \left[\frac{1}{k_{\max\_l}} \sum_{k=1}^{k_{\max\_l}} \exp(-\beta \bar{U}_{ext\_l}(r_k)) \right] \tag{11}$$

where the subscript k refers to test locations, $\bar{U}_{ext\_l}(r_k)$ is the energy increment associated with one additional force centre in location r_k. Once the chemical potential is determined from (10), the determination of the Henry constant in international units follows from (8), in which $\langle N_i \rangle$ is set to unity.

3.5 Heat and entropy of adsorption at low coverage

In this work, the heat of adsorption at low coverage is determined from two methods: calculated using the van 't Hoff equation (method 1) and using the statistical fluctuations in the Grand Canonical ensemble (method 2). For the first method, the heat of adsorption ΔH_0 at low coverage is calculated using the Henry constants K_H obtained by simulation in a temperature range by linear regression of the van 't Hoff equation:

$$K_H = K' \exp\left(\frac{-\Delta H_0}{RT}\right) \tag{12}$$

where K' is the preexponential factor. This procedure is identical to the method used by Denayer and Baron (1997) to obtain heats of adsorption from experimental Henry constants.

With method 2, the heat of adsorption is computed using Grand Canonical Monte Carlo simulation at low coverage ($\langle N \rangle = 2$ to 4 molecules per unit cell) and the simulations lasted for some 10 million steps. The heat of adsorption is computed using fluctuation of energy and of number of molecules by the expression (Pascual et al. 2003):

$$\Delta H_0 = RT - \frac{\langle U^s_{ext} N \rangle - \langle U^s_{ext} \rangle \langle N \rangle}{\langle N^2 \rangle - \langle N \rangle^2} \tag{13}$$

where U^s_{ext} represents intermolecular interactions in the adsorbed phase and N is the number of adsorbed molecules. Care is taken in this procedure to ensure that the average number of molecules in the simulation box is at least 3, otherwise (13) may lead to erroneous results.

The entropy of adsorption $\Delta S_{0,local}$ at low coverage is determined from its relationship with the preexponential factor K' of the van 't Hoff equation, which involves as well the number of adsorption sites n_T through (Denayer and Baron 1997; Denayer et al. 1998)

$$K' = \exp\left[\frac{\Delta S_{0,local}}{R} + \ln\left(\frac{n_T}{2p^\theta}\right)\right] \tag{14}$$

where p^θ is a standard pressure chosen by Denayer et al. as 1 bar.

We expect the cation sites in supercages (sites II in NaY) to represent the adsorption sites for the first adsorbed molecules at low coverage, since the electrostatic field is higher near the cations and also because the sodalite cages are unaccessible to alkanes. The number of cations in sites II being equal to 32 per unit cell in a faujasite $Na_{52}Y$ (Table 3), we considered thus $n_T = 32$ in (14).

4 Results and discussion

4.1 Adsorption isotherms of n-alkanes in Faujasite

Pure component adsorption isotherms of ethane, propane, n-butane, n-octane and n-decane were computed in the temperature range 298 to 598 K (Figs. 2–7). The statistical uncertainties for simulation results are smaller than the symbol size. All alkanes have been observed to fill the supercages only. In order to qualify the high pressure plateau characterizing all adsorption isotherms, we propose to define "saturation" conditions as those prevailing in liquid-vapor equilibrium conditions, i.e. at the saturated vapor pressure of the compound considered at a given temperature. This is justified by the fact that reaching significantly higher fugacities than vapor-liquid equilibrium conditions would correspond

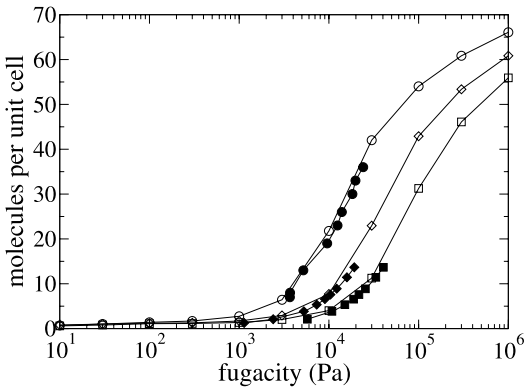

Fig. 2 Adsorption isotherms of ethane in FAU $Na_{56}Y$ (Si:Al = 2.43) at 273 K (*circles*), 298 K (*diamonds*) and 323 K (*squares*) obtained from simulation (*open symbols*) compared with experiments of Hampson and Rees (1993) carried out at the same temperatures (*filled symbols*)

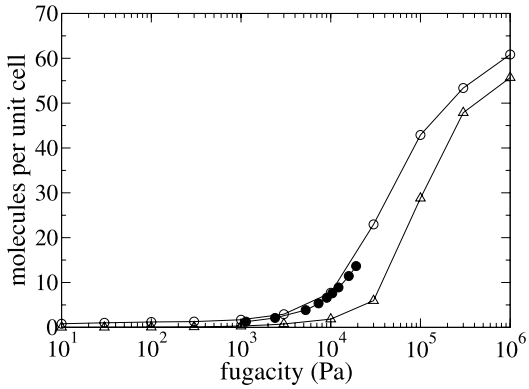

Fig. 3 Adsorption isotherms of ethane in FAU $Na_{56}Y$ (Si:Al = 2.43) at 298 K obtained from simulation with the polarization energy term (*open circles*) and without the polarization energy term (*open triangle*) compared with experiments of Hampson and Rees (1993) carried out at the same temperature (*filled circles*)

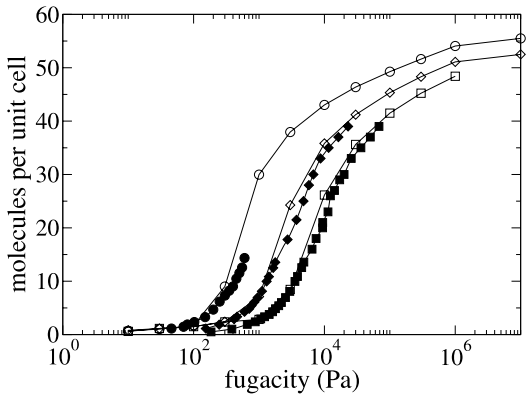

Fig. 4 Adsorption isotherms of propane in FAU $Na_{56}Y$ (Si:Al = 2.43) at 273 K (*circles*), 298 K (*diamonds*) and 323 K (*squares*) obtained from simulation (*open symbols*) compared with experiments of Hampson and Rees (1993) carried out at the same temperatures (*filled symbols*)

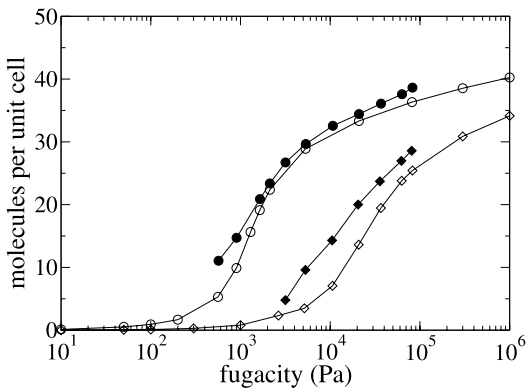

Fig. 5 Adsorption isotherms of n-butane in FAU $Na_{52}Y$ (Si:Al = 2.69) at 343 K (*circles*) and 423 K (*diamonds*) obtained from simulation (*open symbols*) compared with experimental data (this work) carried out at the same temperatures (*filled symbols*)

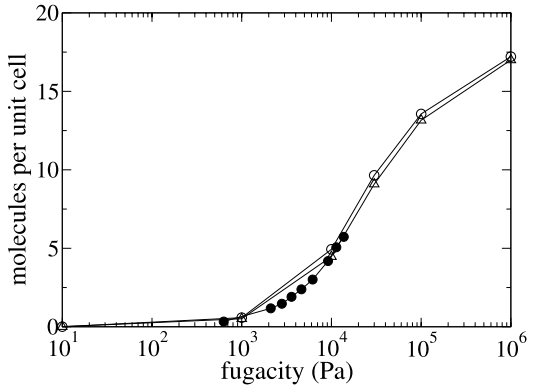

Fig. 6 Adsorption isotherms of n-octane in FAU $Na_{52}Y$ (Si:Al = 2.69) at 548 K obtained from simulations with fixed cations (*open circles*) and with mobile cations (*open triangle*) compared with experiments of Denayer and Baron (1997) at 548 K (*filled symbols*)

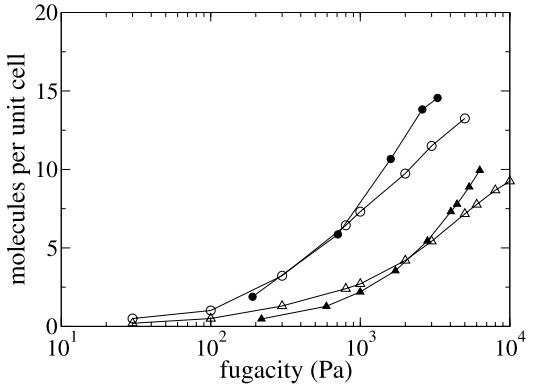

Fig. 7 Adsorption isotherms of n-decane in FAU $Na_{52}Y$ (Si:Al = 2.69) at 548 K (*circles*) and 598 K (*triangles*) obtained from simulation (*open symbols*) compared with experiments of Denayer and Baron (1997) carried out at the same temperatures (*filled symbols*)

to extremely high pressures, since the fugacity of a liquid increases slowly with pressure.

In the case of ethane, simulations have been carried out at 273 K, 298 K and 323 K in zeolite $Na_{56}Y$ (Si:Al = 2.69) and compared with experimental results of Hampson and Rees (1993) (see Fig. 2). Simulations are in very good agreement with experiments at all temperatures. At saturation, we predict 66.1, 60.8 and 55.9 molecules adsorbed per unit cell respectively at 273 K, 298 K and 323 K. In Fig. 3, we have compared the adsorption isotherms of ethane at 298 K in zeolite $Na_{56}Y$ computed with and without the polarization energy term. We see in this example, the significant influence of the polarization energy of alkanes on the adsorption behavior, which permits to improve the results with reference to experimental data.

For propane, the simulations carried out at 273 K, 298 K and 323 K in zeolite $Na_{56}Y$ (Si:Al = 2.43) can be compared with the experimental results of Hampson and Rees (1993) (see Fig. 4). Simulations are in excellent agreement with experimental data. Similarly to the case of ethane, the adsorbed amount in saturation conditions is found to decrease with increasing temperature, as it is 54.1, 51.1 and 48.4 molecules per unit cell respectively at 273 K, 298 K and 323 K.

For n-butane, adsorption isotherms shown in Fig. 5 were computed at 343 K and 423 K in zeolite $Na_{52}Y$. These simulation results were compared with the experimental measurements of Table 1. Simulations are in fair agreement with experiments at 343 K, but underestimate the experimental average number of molecules in the range 10^3–10^5 Pa. At saturation, we predict 40.3 and 34.1 molecules adsorbed respectively at 343 K and 423 K.

For n-octane, adsorption isotherms have been computed at 548 K in zeolite $Na_{52}Y$ and compared with experimental results of Denayer and Baron (1997) either with fixed or mobile sodium cations (Fig. 6). Both simulations are in very good agreement with experimental data. When cation mobility is included in our simulations, the average number of adsorbed molecules decreases by about 6% with reference to simulations with fixed cations. At saturation, we predict 17 molecules adsorbed per unit cell. The influence of alkane adsorption on cation mobility will be more specifically discussed below.

For n-decane, simulated adsorptions were carried out at 548 K and 598 K in zeolite $Na_{52}Y$ and compared with experimental results of Denayer and Baron (1997) (Fig. 7). As convergence of the adsorbed quantities of long alkanes is longer to obtain, we have doubled the number of Monte Carlo steps to 40 millions. For both temperatures, simulations tend to slightly overestimate the adsorbed quantities at low coverage and to underestimate them at high coverage.

The average contribution of the polarization term to the total interaction energy between the guest molecules and the zeolite framework is found to be in the 30–40% range in the cases investigated in our study. This term is must greater that what is obtained in pure silica zeolite: for instance, we found that the polarization account for only 4% in silicalite −1. For example, the polarization energy of adsorbed n-butane in $Na_{52}Y$ at 343 K is −14.2 kJ/mol at 10 Pa (39% of the total energy) and −12.4 kJ/mol at 1.10^6 Pa (32% of the total energy). For the adsorption of n-octane at 548 K, the polarization energy is −16.2 kJ/mol at 10 Pa (35% of the total energy), and −18.3 kJ/mol at 1.10^6 Pa (31% of the total energy). We have noticed that the percentage of the polarization energy over the total energy decreases progressively by some 4–7% from the low coverage regime until the saturation conditions. This behavior can be explained by considering that the adsorbed molecules at low coverage are located near the cations in sites II where the electrostatic field is high and during the course of pore filling, the molecules are located on adsorption sites with a lower polarization energy. However the polarization energy of the latter sites is still significant.

Table 7 Henry constants (mol/kg/Pa) of linear alkanes at 548 K, 598 K and 673 K on faujasite $Na_{52}Y$ (Si:Al = 2.69) compared with experimental data (Denayer and Baron 1997)

Temperature (K)	548		598		673	
K_H (mol/kg/Pa)	This work	Exp	This work	Exp	This work	Exp
Hexane	2.36E-05	2.83E-05	9.92E-06	5.58E-06	3.47E-06	4.42E-06
Heptane	5.43E-05	6.91E-05	2.02E-05	1.31E-05	6.09E-06	8.33E-06
Octane	1.23E-04	1.67E-04	4.04E-05	5.79E-05	1.05E-05	1.59E-05
Nonane	2.84E-04	3.65E-04	4.67E-05	1.14E-04	1.81E-05	2.75E-05
Decane	6.58E-04	1.07E-03	1.66E-04	2.91E-04	3.18E-05	5.94E-05
Undecane	1.59E-03	2.63E-03	3.46E-04	6.35E-04	5.64E-05	1.12E-04
Dodecane	3.77E-03	4.85E-03	7.39E-04	1.08E-03	1.02E-04	1.73E-04

4.2 Cation displacement upon adsorption

We have studied the cation displacement upon octane adsorption in faujasite $Na_{52}Y$ at 598 K. No cation redistribution between different crystallographic sites was observed during adsorption. Cations in sites I, I' and II were however slightly displaced from their initial position in the empty zeolite by 0.11 Å to 0.28 Å. This result is in contrast with the simulation results of Calero et al., who found that the redistribution of cations in faujasites was essential to explain alkane adsorption (Calero et al. 2004). In both models the agreement between simulated and adsorbed quantities and experiments is good (a better agreement is found in the work of Calero, but their force field was specifically adapted for the alkane-faujasite problem). In the force field of Calero et al., the polarization is implicitly taken into account by the dispersion-repulsion potential. As a consequence, it is not surprising that the Lennard-Jones energy parameters involving sodium is much larger in their model than in ours. For instance, the interaction parameters for CH_3-Na and CH_2-Na interactions are 443.73 K and 310 K respectively in Calero's force field, while they are only and 77.77 K and 65.91 K in our model (this follows directly from Table 4 parameters and (5)). In contrast, the Lennard-Jones energetic parameters between alkane groups and the zeolitic framework are closer in magnitude: 93 K and 60.5 K for CH_3-O and CH_2-O interactions respectively in Calero's force field, compared with 106.01 K and 86.59 K for the same interactions in ours. The consequence of these differences is that the implicit account of polarization in Calero's potential is concentrated in the immediate vicinity of cations, because of the rapidly decaying r^{-6} dependence of the Lennard-Jones attraction with separation distance. On the opposite, the explicit polarization in our model is more evenly distributed in the zeolite for two reasons. A first reason is that polarization decays more slowly than dispersion energy with separation distance: the electrostatic field is decreasing like r^{-2} around a point charge such as a cation, so that the polarization energy decreases like r^{-4} according to (7). A second reason is that the framework charges are also contributing to the electrostatic field. It must be kept in mind that the positive charge on cations is compensated by an opposite charge on the framework, so it may be expected that the framework contributes to the polarization energy with a comparable amplitude to the cations as a whole. It is therefore not surprising that Calero and coworkers have found a substantial redistribution of cations in their model, as their interaction with alkanes has been significantly increased compared with the true polarization.

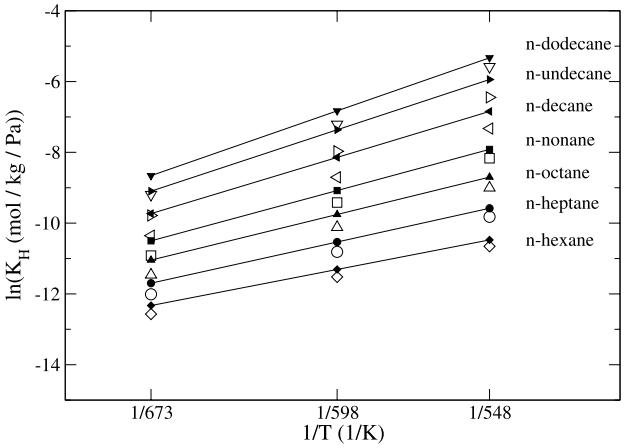

Fig. 8 Henry constants of linear alkanes in sodium faujasite $Na_{52}Y$ (Si:Al = 2.69) obtained from our simulation (*open symbols*) and compared with experimental data (Denayer and Baron 1997) (*lines* and *full symbols*). The statistical uncertainty is smaller than the symbol size

4.3 Henry constants

In this section, we study the validity of our potential model for adsorption in low coverage regime.

The Henry constants of linear alkanes at 548 K, 598 K and 673 K on the faujasite $Na_{52}Y$ are listed in Table 7 and plotted against $1/T$ in Fig. 8. The Henry constants decrease with increasing temperature and number of carbon for linear alkanes. The simulation results are in a good agreement

Table 8 Coefficients A and B of the correlation $K_H = Ae^{BCN}$ between Henry Constants and carbon number for linear alkanes at 548 K, 598 K and 673 K on faujasite $Na_{52}Y$ (Si:Al = 2.69) compared with experimental data (Denayer and Baron 1997)

Temperature (K)	A		B	
	This work	Exp	This work	Exp
548	1.12×10^{-7}	7.47×10^{-7}	0.87	0.73
598	6.84×10^{-7}	4.20×10^{-7}	0.77	0.66
673	1.01×10^{-7}	2.29×10^{-7}	0.58	0.55

Table 9 Average heats of adsorption at low coverage (kJ/mol) of linear alkanes in $Na_{52}Y$ (Si:Al = 2.69) in the temperature range 548–673 K obtained from methods 1 (van 't Hoff) and 2 (fluctuations), compared with experimental data (Denayer and Baron 1997). The subscripts are the estimated statistical uncertainties in kJ/mol

	$-\Delta H_0$ (kJ/mol)		
	Method 1	Method 2	Exp
Hexane	46.9	$45.9_{0.9}$	45.5
Heptane	53.6	$51.6_{1.7}$	51.9
Octane	60.3	$57.8_{0.3}$	57.5
Nonane	67.4	$63.6_{0.2}$	63.4
Decane	74.3	$69.8_{0.1}$	70.8
Undecane	81.8	$75.8_{0.2}$	77.4
Dodecane	88.7	$82.1_{0.2}$	81.7

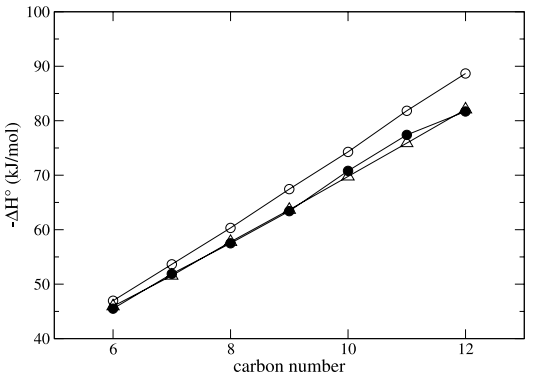

Fig. 9 Heats of adsorption at low coverage (kJ/mol) of linear alkanes calculated using van 't Hoff equation (method 1) (○), using the statistical fluctuations (method 2) (△) and compared with Denayer and Baron (1997) experimental data (●)

Table 10 Relationships between heats of adsorption at low coverage obtained with the methods 1 and 2, and the carbon number of linear alkanes on $Na_{52}Y$ (Si:Al = 2.69) compared with experimental data (Denayer and Baron 1997)

	$-\Delta H_0$ (kJ/mol) $= bCN + c$	
	b	c
Method 1	6.98 ± 0.03	4.77 ± 0.3
Method 2	6.04 ± 0.05	9.47 ± 0.5
Exp	6.18 ± 0.14	8.45 ± 1.3

with experimental data of Denayer and Baron (1997) with a deviation of 2–4% for carbon numbers smaller than 8, and 5–7 % for carbon numbers greater than 8. Denayer and Baron (1997), Denayer et al. (1998) have shown that the Henry constants obey an exponential relationship with carbon number, CN:

$$K_H = Ae^{BCN} \tag{15}$$

where A (mol/kg/Pa) and B are temperature-dependent parameters. The A and B value determined from both experimental and simulation data are given in Table 8.

4.4 Heat of adsorption at low coverage

We have compared the heats of adsorption at low coverage of linear alkanes obtained by methods 1 and 2 with the experimental data of Denayer and Baron (1997) measured in a 548–673 K temperature range. In the case of method 2, we have computed heats of adsorption at three temperatures (548 K, 598 K and 673 K) in the experimental temperature range and we report the average values. The heats of adsorption at low coverage of linear alkanes on $Na_{52}Y$ are given in Table 9 and are shown in Fig. 9. The heats of adsorption calculated using the van 't Hoff equation (method 1) overestimate the experimental values by about 1 kJ/mol for hexane to 7 kJ/mol for dodecane. The average heats of adsorption obtained by method 2 agree better with experimental data with deviations ranging from 0.3 kJ/mol for hexane to 1.6 kJ/mol for dodecane, i.e. 0.7 to 2%. The errors in method 1 simply reflect the overestimation of K_H which increases with temperature (see Fig. 8). The heat of adsorption increases by some 6–8 kJ/mol per additional CH_2-group for the linear chains and is compared with Denayer and Baron (1997) experimental data presenting an increase of 6-7 kJ/mol per extra CH_2-group. A linear relationship between heat of adsorption of linear alkanes (Fig. 9) and the carbon number has been fitted to simulation results and compared with the experimental fit (Table 10):

$$-\Delta H_0 = bCN + c \tag{16}$$

4.5 Preexponential factor

The preexponential factors K' of the van 't Hoff equation are calculated with the heats of adsorption calculated by method 2. The evolution of preexponential factors with carbon number of linear alkanes (Fig. 10, Table 11) can be fitted with a linear relationship:

$$-\ln K' = dCN + e \tag{17}$$

where the d and e parameters are given in Table 12.

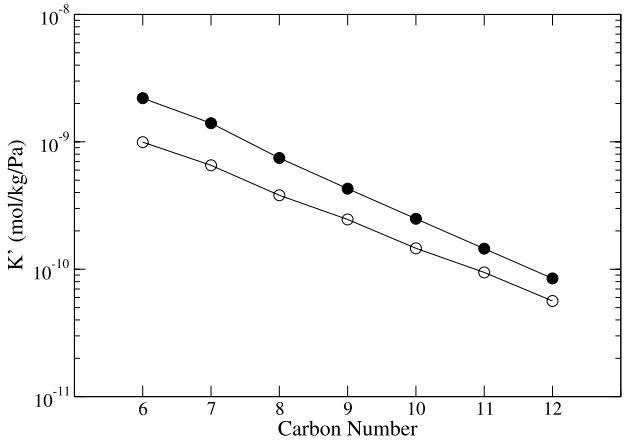

Fig. 10 Preexponential factors of the van 't Hoff equation of linear alkanes, comparison between values obtained by simulation results (*open symbol*) and experimental data (Denayer and Baron 1997) (*full symbol*)

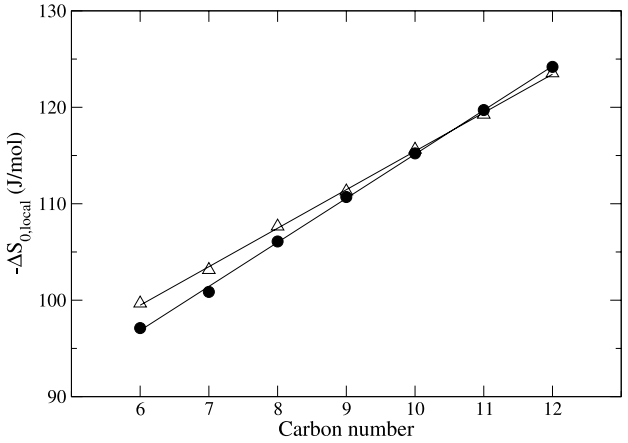

Fig. 11 Localized adsorption entropies of linear alkanes against carbon number at low coverage, comparison between values obtained by simulation results (*open symbol*) and by analysis of experimental data (Denayer and Baron 1997) (*full symbol*)

Table 11 Preexponential Factors of the van 't Hoff Equation and Entropy of adsorption at low coverage of linear alkanes on $Na_{52}Y$ (Si:Al = 2.69) compared with experimental data (Denayer and Baron 1997)

	K' (mol/kg/Pa)		$-\Delta S_{0,local}$ (J/mol)	
	This work	Exp	This work	Exp
Hexane	9.94E-10	2.20E-09	99.7	97.10
Heptane	6.55E-10	1.40E-09	103.1	100.9
Octane	3.81E-10	7.47E-10	107.7	106.1
Nonane	2.46E-10	4.29E-10	111.3	110.7
Decane	1.46E-10	2.48E-10	115.6	115.2
Undecane	9.44E-11	1.45E-10	119.3	119.7
Dodecane	5.63E-11	8.47E-11	123.5	124.2

Table 12 Relationships between preexponential factors and the carbon number of linear alkanes on $Na_{52}Y$ (Si:Al = 2.7) and between entropies of adsorption and the carbon number, compared with experimental data (Denayer and Baron 1997)

	$-\ln K'$ (mol/kg/Pa) $= dCN + e$	
	d	e
This work	0.48 ± 0.005	17.8 ± 0.05
Exp	0.55 ± 0.007	16.6 ± 0.06
	$-\Delta S_{0,local}$ (J/mol) $= gCN + j$	
	g	j
This work	3.99 ± 0.01	75.5 ± 0.4
Exp	4.57 ± 0.04	69.5 ± 0.4

4.6 Adsorption entropy at low coverage

The adsorption entropies of linear alkanes are calculated according to (14) (Table 11). A linear relationship between adsorption entropy and carbon number of linear alkanes is observed in Fig. 11:

$$-\Delta S_{0,local} = gCN + j \tag{18}$$

where g and j parameters are given in Table 12. The stronger interaction of the alkanes with the zeolite framework results in a decrease of their degrees of freedom (translation, rotation). We observed the expected linear relationship between the heat of adsorption and the adsorption entropy (see Fig. 12) when the Gibbs free energy is constant (Atkinson and Curthoys 1981).

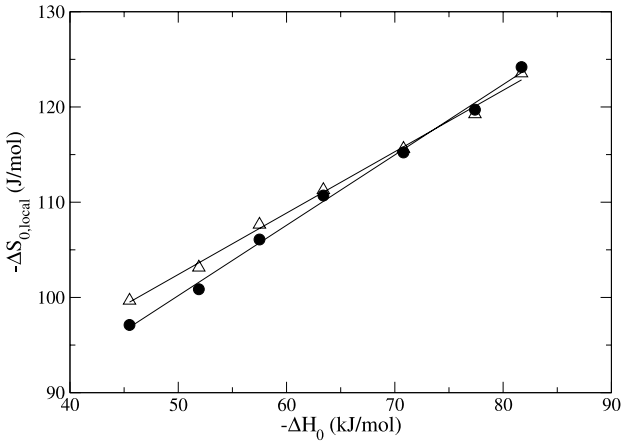

Fig. 12 Relationship between localized adsorption entropies and heats of adsorption at low coverage of linear alkanes, comparison between values obtained by simulation results (*open symbol*) and by analysis of experimental data (Denayer and Baron 1997) (*full symbol*)

5 Conclusion

The proposed extension of Orsay-IFP force field (Pascual et al. 2003) to the adsorption of linear alkanes in sodium faujasite systems makes use of the same framework oxygen Lennard-Jones parameters and it relies similarly on Lorentz–Berthelot combining rules to obtain guest-host cross parameters. In order to extend this force field from siliceous to cationic zeolites, we have shown that an appropriate account of the polarization energy is necessary, as its share ranges between 30 and 40% of the zeolite-molecule interaction energy. In our model the polarization is found as an explicit consequence of the strong electrostatic field created by the sodium cation distribution and by the negatively charged framework. A first order polarization term is explicitly used to introduce this contribution in grand canonical Monte Carlo simulations.

Thanks to the original n-butane adsorption isotherms measured in the present study, we could complement the available adsorption isotherms of ethane, propane, n-octane and n-decane to evaluate the force field for a large range of alkanes in NaY faujasite. These tests have been extended to Henry constants and heats of adsorption at zero coverage for n-alkanes ($n = 6$–10). The general agreement between simulation results and experiments ranged from fair to excellent, from a qualitative as well as from a quantitative standpoint. This result may be considered remarkable, as it was obtained without any specific parameter calibration. In contrast to the work of (Calero et al. 2004), we do not find an important influence of cation mobility on alkane adsorption isotherms nor a significant redistribution of cations upon alkane adsorption. The redistribution of cations found by Calero and coworkers is presumably due to the implicit attribution of polarization interactions to very short range cation-alkane interactions in their model.

Further application of the proposed model to other molecules, like branched of cyclic alkanes, and to other aluminium-substituted zeolites appears straightforward. Moreover, the proposed evaluation of polarization energy is fully consistent with our previous treatment of coulombic interactions in the simulation of polar molecules like water (Beauvais et al. 2004) and alkanethiols (Ungerer et al. 2005). An interesting perspective, among others, is to apply the proposed force field to the complex interplay of water adsorption, cation mobility and alkane adsorption.

References

Abdul-Rehman, H.B., Hasanain, N.A., Loughlin, K.F.: Quaternary, ternary, binary, and pure-component sorption on zeolites. 1. Light alkanes on Linde S-115 silicalite at moderate to high pressures. Ind. Eng. Chem. Res. **29**, 1525 (1990)

Atkinson, D., Curthoys, G.: Heats and entropies of adsorption of saturated hydrocarbons by zeolites X and Y. J. Chem. Soc. Faraday Trans. 1 **77**, 897 (1981)

Beauvais, C., Guerrault, X., Coudert, F.-X., Boutin, A., Fuchs, A.H.: Distribution of sodium cations in faujasite-type zeolite: a canonical parallel tempering simulation study. J. Phys. Chem. B **108**, 399 (2004)

Beerdsen, E., Smit, B., Calero, S.: The influence of non-framework sodium cations on the adsorption of alkanes in MFI- and MOR-type zeolites. J. Phys. Chem. B **106**, 10659 (2002)

Beerdsen, E., Dubbeldam, D., Smit, B., Vlugt, T.J.H., Calero, S.: Simulating the effect of nonframework cations on the adsorption of alkanes in MFI-type zeolites. J. Phys. Chem. B **107**, 12088 (2003)

Bourasseau, E., Ungerer, Ph., Boutin, A., Fuchs, A.H.: Monte Carlo simulation of branched alkanes and long chain n-alkanes with anisotropic united atoms intermolecular potential. Mol. Simul. **28**, 317 (2002a)

Bourasseau, E., Ungerer, Ph., Boutin, A.: Prediction of equilibrium properties of cyclic alkanes by Monte Carlo simulation—new anisotropic united atoms potential—new transfer bias method. J. Phys. Chem. B **106**, 5483 (2002b)

Bourasseau, E., Haboudou, M., Boutin, A., Fuchs, A.H., Ungerer, Ph.: New optimization method for intermolecular potentials—optimization of a new anisotropic united atoms potential for olefins—prediction of equilibrium properties. J. Chem. Phys. **118**, 3020 (2003)

Boutin, A., Buttefey, S., Fuchs, A.H., Cheetham, A.K.: Molecular simulation of adsorption of guest molecules in zeolitic materials: a comparative study of intermolecular potentials. Mol. Simul. **27**, 371 (2001)

Boyd, R.H.: An off-lattice constant-pressure simulation of liquid polymethylene. Macromolecules **22**, 2477 (1989)

Calero, S., Dubbeldam, D., Krishna, R., Smit, B., Vlugt, T.J.H., Denayer, J.F.M., Martens, J.A., Maesen, T.L.M.: Understanding the role of sodium during adsorption: a force field for alkanes in sodium-exchanged faujasites. J. Am. Chem. Soc. **126**(36), 11377 (2004)

Dang, L.X.: Mechanism and thermodynamics of ion selectivity in aqueous solutions of 18-crown-6-ether—a molecular dynamics study. J. Am. Chem. Soc. **117**, 6954 (1995)

Delhommelle, J., Millié, P., Fuchs, A.H.: On the role of the definition of potential models in Gibbs ensemble simulations of the H2S-n-pentane mixture. Mol. Phys. **98**, 1895 (2000)

Denayer, J.F.M., Baron, G.V.: Adsorption of normal and branched paraffins in faujasite NaY, HY, Pt/NaY and USY. Adsorption **3**, 251 (1997)

Denayer, J.F.M., Souverijns, W., Jacobs, P.A., Martens, J.A., Baron, G.V.: High-temperature low-pressure adsorption of branched C5-C8 alkanes on zeolite beta, ZSM-5, ZSM-22, zeolite Y, and mordenite. J. Phys. Chem. B **102**, 4588 (1998)

Dubbeldam, D., Calero, S., Vlugt, T.J.H., Krishna, R., Maesen, T.L.M., Smit, B.: United atom force field for alkanes in nanoporous materials. J. Phys. Chem. B **108**, 12301 (2004)

Fitch, A.N., Jobic, H., Renouprez, A.: Localization of benzene in sodium-Y zeolite by powder neutron diffraction. J. Phys. Chem. **90**, 1311 (1986)

Frenkel, D., Smit, B.: Understanding Molecular Simulation. From Algorithms to Applications. Academic, San Diego (1996)

Fuchs, A.H., Cheetham, A.K.: Adsorption of guest molecules in zeolitic materials: computational aspects. J. Phys. Chem. B **105**, 7375 (2001)

Gener, I., Buntinx, G., Bremart, C.: Sorption of biphenyl in non-acidic MFI-type zeolites: spectroscopic and modelling studies. Microporous Mesoporous Mater. **41**, 253 (2000)

Hampson, J.A., Rees, L.V.C.: Adsorption of ethane and propane in Silicalite-1 and zeolite NaY: determination of single compo-

nents, mixture and partial adsorption data using isosteric system. J. Chem. Soc. Trans. **89**, 3169 (1993)
Jaramillo, E., Auerbach, S.M.: New force field for Na cations in faujasite-type zeolites. J. Phys. Chem. B **103**, 9589 (1999)
Lachet, V., Boutin, A., Tavitian, B., Fuchs, A.H.: Computational study of p-xylene/m-xylene mixtures adsorbed in NaY zeolite. J. Phys. Chem. B **102**, 9224 (1998)
Lachet, V., Boutin, A., Tavitian, B., Fuchs, A.H.: Molecular simulation of p-xylene and m-xylene adsorption in Y zeolites, single components and binary mixtures study. Langmuir **15**, 8678 (1999)
Lachet, V., Buttefey, S., Boutin, A., Fuchs, A.H.: Molecular simulation of adsorption equilibria of xylene isomer mixtures in faujasite zeolites. A study of cation exchange effect on adsorption selectivity. Phys. Chem. Chem. Phys. **3**, 80 (2001)
Loyens, L.D.J.C., Smit, B., Esselink, K.: Parallel Gibbs-ensemble simulations. Mol. Phys. **86**, 171 (1995)
Marantzas, V.G., Theodorou, D.N.: Atomistic simulation of polymer melt elasticity: calculation of the free energy of an oriented polymer melt. Macromolecules **31**, 6310 (1998)
Mellot, C.F., Cheetham, A.K.: Energetics structures of fluoro- and chlorofluorocarbons in zeolites: force field development and Monte Carlo simulations. J. Phys. Chem. B **103**, 3864 (1999)
Pablo, J.J., Laso, M., Suter, U.W.: Simulation of polyethylene above and below the melting point. J. Chem. Phys. **96**, 2395 (1992)
Pascual, P., Pernot, P., Ungerer, Ph., Tavitian, B., Boutin, A.: Development of a transferable guest-host force field for adsorption hydrocarbons in zeolites. Reinvestigation of alkanes adsorption in silicalite by grand canonical Monte Carlo simulation. Phys. Chem. Chem. Phys. **5**, 3684 (2003)
Pascual, P., Boutin, A., Ungerer, Ph., Tavitian, B., Fuchs, A.H.: Adsorption of hydrocarbons in zeolites from molecular simulations. The alkane–ferrierite system revisited. Chem. Phys. Chem. **6**, 2015 (2004)
Pascual, P., Kirsch, H., Boutin, A., Paillaud, J.-L., Soulard, M., Tavitian, B., Faye, D., Fuchs, A.H.: Adsorption of various hydrocarbons in siliceous zeolites: a molecular simulation study. Adsorption **11**, 379 (2005)
Ramachandran, C.E., Williams, B.A., van Bokhoven, J.A., Miller, J.T.: Observation of a compensation relation for n-hexane adsorption in zeolites with different structures: implications for catalytic activity. J. Catal. **233**, 100 (2005)
Smit, B., Maesen, T.L.M.: Commensurate freezing of alkanes in the channels of a zeolite. Nature **374**, 42 (1995)
Smit, B., Siepmann, I.J.: Computer simulations of the energetics and siting of n-alkanes in zeolites. J. Phys. Chem. **98**, 8442 (1994)
Smit, B., Karaborni, S., Siepmann, I.J.: Computer simulation of vapor-liquid phase equilibria of n-alkanes. J. Chem. Phys. **102**, 2126 (1995)
Stach, H., Lohse, U., Thamm, H., Schirmer, W.: Adsorption equilibria of hydrocarbons on highly dealuminated zeolites. Zeolites **6**, 74 (1986)
Sun, M.S., Shah, D.B., Xu, H.H., Talu, O.: Adsorption equilibria of C1 to C4 alkanes, CO2, and SF6 on silicalite. J. Phys. Chem. B **102**, 1466 (1998)
Ungerer, Ph., Beauvais, C., Delhommelle, J., Boutin, A., Rousseau, B., Fuchs, A.H.: Optimization of the anisotropic united atoms intermolecular potential for n-alkanes. J. Chem. Phys. **112**, 5499 (2000)
Ungerer, Ph., Tavitian, B., Boutin, A.: Applications of Molecular Simulation in the Oil and Gas Industry—Monte Carlo Methods. Editions Technip, Paris (2005)
Uytterhoeven, L., Dompas, D., Mortier, W.J.J.: Theoretical investigations on the interaction of benzene in faujasite. Chem. Soc. Faraday Trans. **18**, 2753 (1992)
Vacatello, M., Avitabile, G., Corradini, P., Tuzi, A.: A computer model of molecular arrangement in a n-paraffinic liquid. J. Chem. Phys. **73**, 548 (1980)
Vitale, G., Mellot, C.F., Bull, L.M., Cheetham, A.K.: Neutron diffraction and computational study of zeolite NaX: influence of SIII' cations on its complex with benzene. J. Phys. Chem. B **101**, 4559 (1997)